SCIENCE CHINA
Physics, Mechanics & Astronomy

• Article •

July 2015 Vol. 58 No. 7: 077001
doi: 10.1007/s11433-015-5662-y

Effect of hydrogen on grain boundary migration in tungsten

YU Yi[1], SHU XiaoLin[1], LIU YiNan[1], NIU LiangLiang[1], JIN Shuo[1], GAO Fei[2] & LU GuangHong[1*]

[1] *Department of Physics, Beihang University, Beijing 100191, China;*
[2] *Department of Nuclear Engineering and Radiological Science, University of Michigan, Ann Arbor, MI 48109, USA*

Received January 05, 2015; accepted February 28, 2015; published online April 7, 2015

Motivated by a grain boundary (GB) healing mechanism that GB turns into a mobile sink through migration to eliminate the vacancies in a bulk, we have further investigated the influence of the retained hydrogen (H) on the GB migration in tungsten using a molecular dynamics simulation. We show that H hinders the GB migration at different H concentrations and temperatures, and such friction of GB migration due to the presence of H increases with the H concentration and decreases with temperature. We demonstrate that H follows the GB-migration as the temperature is higher than 300 K. Most importantly, the presence of H induces a disordering of GB, which affects the GB migration significantly.

tungsten grain boundary, hydrogen, migration, molecular dynamics, disordering

PACS number(s): 28.52.Fa, 61.72.Mm, 61.82.Bg, 31.15.Qg

Citation: Yu Y, Shu X L, Liu Y N, et al. Effect of hydrogen on grain boundary migration in tungsten. Sci China-Phys Mech Astron, 2015, 58: 077001, doi: 10.1007/s11433-015-5662-y

1 Introduction

Grain boundaries (GBs) play a quite important role in many processes of materials, including plastic deformation [1] and grain growth [2]. Particularly, the GBs are known to be sinks of vacancies, self-interstitial atoms (SIAs) and other impurities [3]. In nuclear materials, the concentration of point defects which is induced by neutron irradiation, such as vacancies and SIAs, is very high. Bai et al. [4] recently proposed a GB self-healing mechanism that GBs can annihilate the nearby vacancies by re-emitting interstitials from itself in bulk copper under neutron radiation. Unfortunately, the effective interaction distance between GB and vacancies is very short (< 20 Å) [5]. Consequently, if one wants to take advantage of the GB self-healing effect, the distance between vacancies and GB must be shorter than the effective interaction distance. Thus, Ackland [6] proposed that a nano-crystalline material with a very high density of GBs can improve the radiation resistance. Yet by now, the fabricating processes of nano-crystalline material applied in fusion reactor are still not suitable for industrial-scale products [7]. However, an alternative approach may be considered to eliminate the vacancies accumulated under irradiation. Borovikov et al. [8] suggested that the SIAs filled GB can migrate in tungsten (W) under the fusion reactor conditions.

We can consider to utilize the GB migration to sweep the vacancies far away from the GB plane in the metallic materials. GB can migrate with the translation of grains if the shear stress is applied on the metallic materials and such GB migration may be defined as the coupled motion [8–10]. The common GB migration without stress is dominated by the diffusion of vacancies [11], and the coupled motion of GB is dominated by the collective movement of atoms [12]. The coupled motion has a lower migration barrier and higher migration speed compared with the common GB migration. Moreover, the SIAs can reduce the friction of the GB

*Corresponding author (email: lgh@buaa.edu.cn)

migration for some specific type of GB [8]. Under the fusion conditions, the normal heat load is 5–10 MW/m^2, while the transient heat load can reach as high as several hundred MW/m^2 and even GW/m^2 with edged local modes (ELMs) and vertical displacement events (VDEs) [13]. It is very likely that the high transient heat load can lead to the GB migration at a GPa level, consistent with the experimental observations [14]. It is thus probable that GB can be driven to migrate by a large stress field due to such high thermal shock.

In fusion reactor, W has been proposed to be the most promising candidate for the plasma facing materials [15] due to its high melting point, low sputtering rate and low hydrogen (H) or helium (He) solubility. Besides the SIAs and the vacancies, H will also be retained in W in fusion reactor environment. The behaviors of H in W as well as other structural materials have been widely investigated with various computational approaches [16–27] and experimental techniques [7,28–36]. The defects in W, such as vacancies [20,37], dislocations [38] and GBs [18,19], have been shown to be responsible for the H bubble formation, which have systemically been reviewed from modeling and simulation point of view [24]. In addition, H atoms are shown to prefer to segregate into the GB region, instead of staying in the bulk, and H bubbles are most likely to form at GBs [39]. Here, we explore the effects of H on the GB migration under a shear stress with different conditions using a molecular dynamics method, which we hope will provide a helpful reference for the possible self-healing effect in W under a fusion environment.

2 Simulation methods

Here, we employ the molecular dynamics code LAMMPS [40] and a Tersoff-style potential developed by Li [41] for the W-H system. This potential behaves well in terms of defect formation energies, structure properties and the activation energies for H diffusion. A bicrystal model containing a Σ5(310) ⟨001⟩ θ=36.87° symmetric tilt GB is constructed under the coincidence site lattice (CSL) framework. The periodic boundary conditions are imposed along the [310] and [001] directions as shown in Figure 1.

In the *y* direction shown in Figure 1, a fixed boundary condition is adopted to avoid the GB-GB interaction. Grains are sandwiched between two slabs which are set to be semi-rigid. The thickness of each slab is 10 Å, twice the W-W cutoff distance of the potential. The simulation box is 40 Å×200 Å×13 Å and consists of 6432 atoms. The structure of GB has been optimized by the γ-surface search and is no longer mirror symmetry along the *y* direction [42].

The coupled motion is studied by applying a shear stress on the simulation box. There are two common methods to apply the shear stress, the constant strain method and the constant stress method. Here, we employ the constant strain

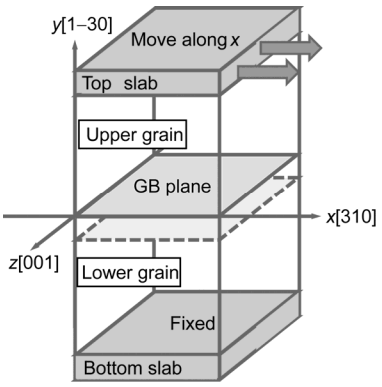

Figure 1 Σ5(310) ⟨001⟩ GB model, where the [001] axis is the tilt axis. The GB plane is located between the upper grain and the lower grain. The top and the bottom slabs are both set to be semi-rigid. To apply shear strain, the top slab is moved at a constant velocity along the *x* direction and the bottom slab is fixed. The simulation box is 40 Å×200 Å×13 Å and consists of 6432 atoms.

method because the constant stress method will cost a lot of time to search the stress to drive the GB migration. The constant strain condition is applied by fixing the bottom slab and imposing a constant velocity on the top slab along the *x* direction (Figure 1). Thus, the top slab will drag the neighboring atoms to move, leading to the shear deformation. It should be noted that the atoms in slabs are all fixed in their perfect lattice sites, and these atoms do not contribute to the calculation of thermal dynamics variables, such as the stress tensor. Other atoms in the simulation box are free to move. Shear stress is employed to identify the deformation of lattice, and such shear stress is calculated by summing all single atom stresses as:

$$\sigma = \frac{1}{V}\left(\sum_i m_i v_i \otimes v_i + \frac{1}{2}\sum_{i,j\neq i} r_{ij} \otimes f_{ij}\right), \quad (1)$$

where V is the volume of the simulation box, m_i is the mass of atom i, v_i is the velocity of atom i, f_{ij} is the force between atom i and atom j, and r_{ij} is the position vector. The first term of this expression represents the kinetic energy contribution and the second term is the virial contribution. The virial term is dominant in the present simulations with the condition of higher stress and relatively low temperature.

A general GB region is defined as a region with the borders about 15 Å from the GB plane, since the formation energy of SIA in this region is slightly different from that in bulk. We also define a smaller GB region with the borders only 3 Å from the GB plane, which is an effective trapping distance of H for the present GB. The H atoms are inserted in the general GB region and the H concentration is determined by the atomic ratio of H to W in the smaller GB region. The H concentration ranges from 1 at.% to 50 at.%, corresponding to the H concentration from 0.01 at.% to 0.5 at.% with consideration of the whole system. Such concen-

tration is actually not high, because most of the H atoms will segregate into the local GB region, making the H concentration reach a higher level. On the other hand, the H concentration can reach 10 at.% at surface and sub-surface region of W based on the experimental observation [28].

Before loading the shear strain, we employ the NPT ensemble to relax the pressure of the system for 50 ps at each temperature, where the two surfaces along the *y*-direction are free to move during this process, and then perform the shear deformation using the NVT ensemble. However, it should be noticed that there still remains small residual stress in the system after the relaxation process. For example, after a relaxation at 600 K, the residual stress along *x* and *z* directions are about 0.1 GPa owing to the thermal fluctuation, which can be considered as zero pressure for the present system. As for the *y* direction, a non-periodic boundary condition has been applied so that the shear deformation can be performed, leading to a relatively high stress of 0.5 GPa. The GB structure is shown to be not symmetric along the *y* direction, as mentioned before. This may be the reason of the relatively high stress at *y* direction. As long as the shear deformation is applied, the stress will be accumulated because the NVT ensemble is employed but not the NPT anymore. Moreover, H atoms will spontaneously segregate towards the GB plane during the relaxation process. During the shear process, the NVT ensemble employing the Nose-Hoover thermostat is applied to control the system temperature and volume.

3 Results and discussion

3.1 Migration of a pure W GB

The coupled motion of GB is a collective motion of atoms in GB [12]. With the translation of upper grain along the *x* direction, the GB will acquire a negative velocity perpendicular to the GB plane in the *y* direction, as shown in the red arrow of Figure 2(a).

The stress varies periodically with the movement of top slab and the displacement of GB behaves as a stick-slip style. At the beginning, the top slab drags the neighboring atoms to move, which is accompanied by an increase of shear stress. The stress wave finally arrives at the GB plane and forces the atoms in the GB plane to move. When the shear stress reaches a critical value, the atoms in the GB plane are displaced from their original positions. At this point, the upper grain and the atoms in the GB plane start to move to new positions along the *x* direction. The atoms in the original GB plane quickly bond with the atoms in the lower layer and form a new GB plane. Thus, the stress is released, which results in the GB migration (Figure 2(b)). Such stick-slip GB behavior and saw-tooth shaped stress-time curve are also reported by the previous work [9,43]. The coupling factor β is a geometric factor that equals to the ratio of the translational distance of grain to the displacement of GB. The β of the $\Sigma5(310)$ symmetric tilt GB equal to 1, namely the translational distance of grain and the displacement of GB are the same. The displacement of GB in one period is determined by the stress and the translation of the top slab. Normally, the top slab drags the atoms in the GB plane to move, so the translational distance of the top slab should be larger than the displacement of GB as the shear stress increases. The inter-layer distance along the *y* axis is 1 Å, and thus, the displacement of GB should be the integer multiples of 1 Å. It is shown in Figure 2(b) that the displacement of GB in one period is 2 Å at 1 K.

Here, we define the absolute value of maximum shear stress in the whole shearing process as a critical stress instead of the average of maximal stresses at each period for the GB migration. The critical stress is shown to increase with the increasing strain rate (Figure 3(a)), but decrease

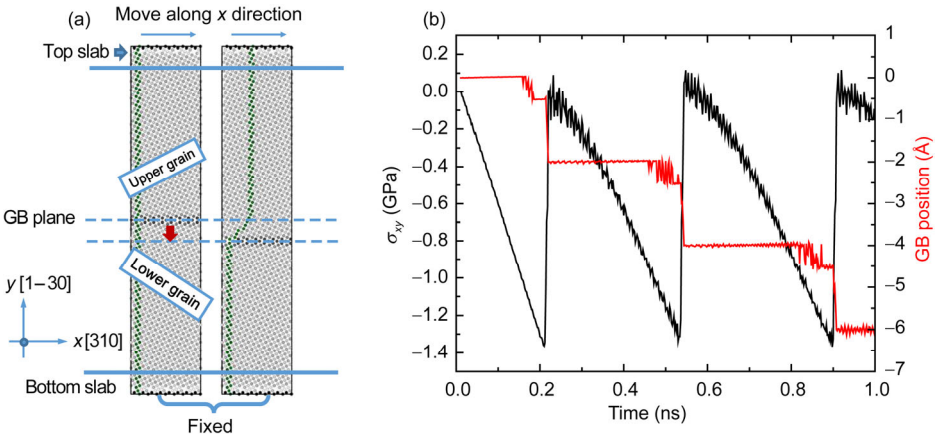

Figure 2 (Color online) Illustration of the coupled motion. (a) Snapshots of the migration of GB, where the atoms with *x* coordinate of 3 Å are colored by green to indicate the trajectories of atoms involved in the migration of GB. (b) The variation of shear stress and the displacement of GB during the migration of GB. Red, stair-shaped line indicates the displacement of GB and the saw-tooth shaped line represents the shear stress. The simulation is performed at a temperature of 1 K and a strain rate of 1 m/s.

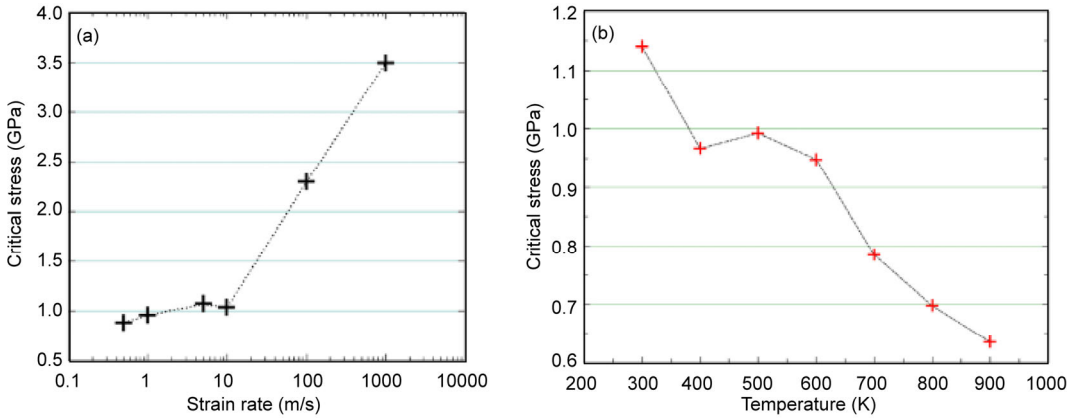

Figure 3 (Color online) The critical stress as a function of (a) strain rate with a temperature of 10 K and (b) temperature with a strain rate of 1 m/s for the GB migration of W.

with the increasing temperature (Figure 3(b)). This is consistent with our previous study [44] via a different W-W potential [45], where we discussed explicitly the dependence of the critical stress on temperature.

When the temperature is above 1000 K, the thermal stress fluctuation will exceed the stress variation caused by the GB migration. The simulations are thus carried out only at the temperature range from 0 K to 900 K. In addition, the critical stress is found quite insensitive to the strain rate in the low strain rate region (0.5–10 m/s). Thus, a constant strain rate of 1 m/s is used in the following simulations.

3.2 Effects of single H on the GB migration

The H atom is first randomly inserted at a position 7 Å away from the GB plane at the beginning to avoid the H atom segregation into the GB plane. Then, a constant strain rate is applied to the top slab. The simulation is performed under a wide temperature range from 10 K to 900 K, and all the other simulation conditions are the same as those in sect. 3.1.

For the low temperature region of 10 K to 300 K, the GB and H atom move separately. Figure 4 illustrates the potential energy, the position of the GB plane, H and the top slab, the shear stress as a function of time at a temperature of 10 K and a strain rate of 1 m/s. As shown in Figure 4(b), after applying the strain on the top slab, the GB starts to migrate along the *y* direction and approach to the single H atom that stays still. When the H atom is about 2 Å away from the GB plane, it jumps towards the GB plane.

To clearly show the effect of H on the GB migration, we divide this shearing process into three stages, i.e. the H atom is (1) in front of the GB plane, (2) in the GB plane and (3) behind the GB plane. In the stage (1), the shearing process is interfered by the H atom. In the first period, the GB migrates a distance of 3 Å and the top slab translates a distance of 2.5 Å. It turns out that GB migrates faster than the slab, leading to the reversed shear stress on the system.

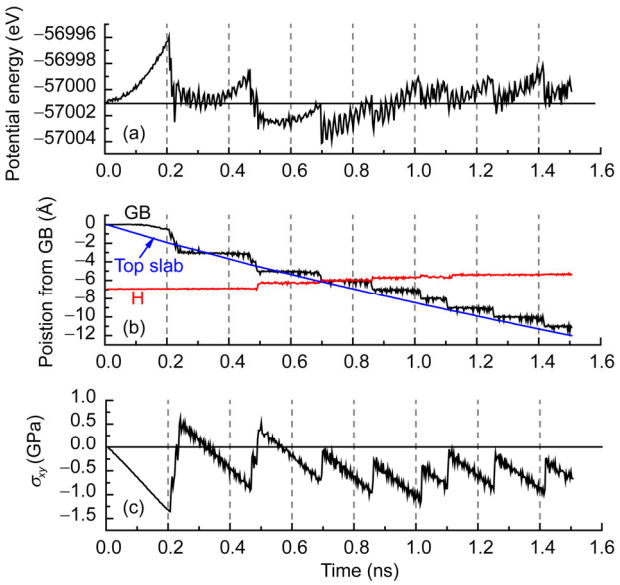

Figure 4 (Color online) (a) The potential energy, (b) the position (GB plane, H and top slab), and (c) the shear stress as a function of time. The simulation is performed at a temperature of 10 K and a strain rate of 1 m/s.

When the H atom gets sufficiently close to the GB plane, it jumps towards the GB plane. This is attributed to the attractive interaction between the GB and the H atom since the GB plane is an energetically favorable site for H. In the stage (2) with the H atom in the GB plane, the H atom moves within the GB plane. In the stage (3), it is of interest to note that the GB continuously migrates, but the H atom does not follow the GB movement. Moreover, the shear stress of the system is not able to drop to 0 GPa since the H atom pins some nearby W atoms of the GB. The potential energy of system (Figure 4(a)) shows a same tendency of variation as the stress. The potential energy with H at the GB plane is lower than that without H at the GB plane by 2.5 eV, and it decreases with H approaching the GB mainly because of the decreasing solution energy of H. Such H-GB interaction leads to the next two migration periods of GB

deviating from the normal GB migration, and the migration distance in these periods becomes shorter, from 2–3 Å to 1 Å.

At a higher temperature of 600 K, despite the original H position is the same as that at 10 K, the H atom spontaneously migrates to the GB plane without the applied strain and the H atom follows the GB migration with the applied strain. In this case, the fluctuation is rather large. The amplitude of the fluctuation reaches 3–4 eV, and the H-GB interaction cannot be distinguished from the thermal fluctuation of system. This is why we did not give the variation of potential as a function of time at 600 K in Figure 5. The incomplete release of stress at 0.25, 0.65, 1.16 and 1.28 ns in Figure 5(a) shows the pining effect of the H atom on the migration of GB. Since the H atom moves along with the GB migration, it will continuously interfere the GB migration, resulting in an increase of the friction of the GB motion.

Thorough investigations of the whole temperature range reveal that the H atom moves along with the GB when the temperature is higher than 300 K, and the H atom and the GB move separately when the temperature is below 300 K. At 300 K, both migration behaviors with and without H-following are observed, implying that the temperature of 300 K is a critical temperature for its migration modes to cross over.

In order to further study the temperature effect, we focus on the motion of the H atom. The diffusion coefficient of an H atom in a cubic metal can be written as [46]:

$$D = \frac{l^2}{6\tau}, \tag{2}$$

where D is the diffusion coefficient, l is the length of H jump in bcc W, which equals to the distance between two nearest-neighbor tetrahedral interstitial sites, and τ^{-1} is the mean atomic jump rate in any direction on a lattice site. Then we can calculate the average velocity of the H as:

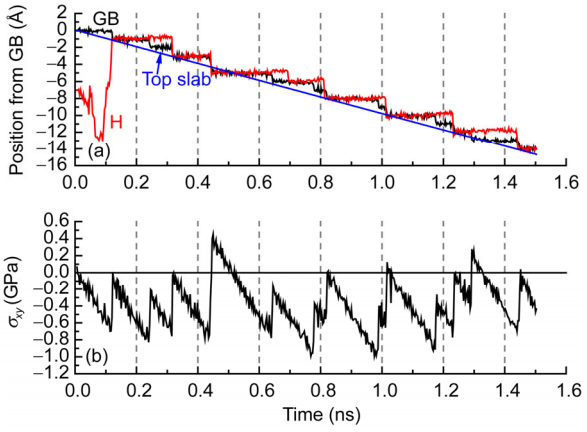

Figure 5 (Color online) The time evolution of (a) the position of GB, H and the top slab and (b) the shear stress. The simulation is performed at a temperature of 600 K and a strain rate of 1 m/s.

$$v_H = \tau^{-1} l = \frac{6D}{l}. \tag{3}$$

For an H atom in bulk W, the bulk diffusion coefficient is determined by

$$D = D_0 \exp(-G/k_B T), \tag{4}$$

where D_0 is the pre-exponential factor, G is the diffusion barrier, k_B is the Boltzmann constant and T is temperature. The velocity of the GB migration is calculated by

$$v_{GB} = \beta v_{slab} = 1 \times v_{slab} = v_{slab} = 1 \quad \text{m/s}. \tag{5}$$

Assuming that v_H equals to v_{GB}, we can determine a critical temperature when the H and the GB have the same velocity,

$$T_d = \frac{G}{k_B}(\ln(6D_0) - \ln(v_{GB} l))^{-1} = 423 \quad \text{K}, \tag{6}$$

where $G = 0.167$ eV, $D_0 = 0.17 \times 10^{-8}$ [47] and $l = 1.12 \times 10^{-10}$ m. It is worth noticing that here we use the H bulk diffusion coefficient to calculate the jump rate τ^{-1}, while in the GB region the diffusion is mainly limited in the y direction and the diffusion coefficient is higher than that in bulk. Hence, the actual T_d for H in the GB region should be lower than that in the present calculation. If the system temperature is higher than T_d, the H atom will move faster than the GB, which results in the H atom moving along with the GB. On the contrary, if the system temperature is lower than T_d, the H atom moves separately from the GB. As compared with the critical value of 300 K obtained from the present simulation, the value of 423 K from the diffusion model is reasonable. In a fusion reactor, the operating temperature is 900 K, at which the v_H is estimated to be 10 m/s. If the velocity of the GB migration is lower than 10 m/s, the H atoms can move along with the GB migration, leaving undamaged lattice behind.

3.3 Effect of H concentration on the GB migration

Now we investigate the influence of multiple H atoms on the GB structure and migration at the temperature of 600 K. As shown in Figure 6, the critical stress for the GB migration increases with H concentration in the GB region. When the H concentration is lower than 13 at.%, the critical stress increases monotonically with the H concentration. However, when the H concentration is higher than 13 at.%, there is no clear dependence between the critical stress and the H concentration. We analyzed the trajectories of atoms and found that when the H concentration was high, the structure of GB turned to be disordered, as shown in the inset of Figure 6 with 17 at.% of H.

Figure 7 shows the dynamic process of the lattice disor-

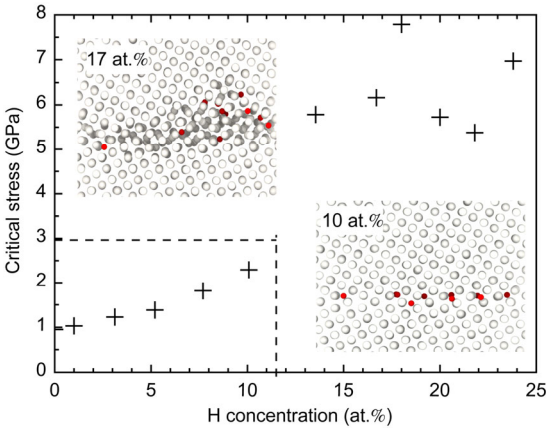

Figure 6 (Color online) Critical stress for the GB migration as a function of H concentration in the GB region. The snapshots of the GB structure after the shear deformation for the H concentrations of 10 at.% and 17 at.% are also shown in the insets. All these simulations are performed at a temperature of 600 K and a strain rate of 1 m/s.

dering caused by the H atoms with a concentration of 17 at.% in the GB region, where a perfect GB crystal is demonstrated as a reference in Figure 7(a). After the strain is applied on the top slab, one W atom on the GB plane (layer 0) is displaced first from its original site by two nearby H atoms and forms an self-interstitial atom (SIA, red open circle in Figure 7(b)) on layer 1. It should be noticed that an SIA can only exist in bulk as a dumbbell or a crowdion structure because there is not enough space to contain an SIA in a common interstitial site. While in the GB region, the SIA can stay in some special interstitial without forming the dumbbell or crowdion. When the GB plane migrates, the W atoms on and above the GB plane will move towards the positive x direction. Then the SIA on layer 1 occupies a common interstitial site and force an atom on layer 2 to move to layer 3. Thus the second SIA forms (red open circle in Figure 7(c)). The formation of the third SIA follows the same mechanism as the first two SIAs (Figure 7(d)). As the GB continuously migrates, more and more SIAs are formed in the GB region (Figure 7(e)) and those SIAs form a disordered structure as shown in Figure 7(f).

As shown in Figure 7, the potential energy of system increases by 9 eV with the GB structure deformation from (a) to (b), and remains unchanged from (b) to (c), while it even decreases by 3 eV from (c) to (d). For both (e) and (f), the potential energy increases by about 30 eV as compared to that of the normal GB structure without SIAs. In general, one SIA can increase the system potential energy by about 9 eV which is approached to the formation energy of one SIA in bulk. Once the first SIA forms in the GB plane, a cascading SIA formation is initiated by the continuing migration of the GB. We also noticed that the formation of the first SIA is closely associated with the H atoms implying that the formation of the first SIA results from the synergistic effect of multiple H atoms. A similar extrusion mechanism of vacancies in W induced by the H atoms is also discussed in the previous work [16], which shows a synergistic effect of H atoms in the coupling formation of vacancies and SIAs. And in certain case with enough SIAs, the SIAs should form energetically favorable ordered clusters. At certain H concentration (critical concentration to the transition—about 13 at.% in the present study), the H atoms have higher probability to aggregate so that an SIA can be extruded out. From atomic configuration analysis, the transition in the critical stress is closely associated with the disordering occurred at the critical stress. Moreover, the atomic density of GB is lower than in the bulk, so the self-interstitial atom is easier to form due to the weak atomic bonding, and thus the critical H concentration to form SIAs in the GB is also lower than in the bulk.

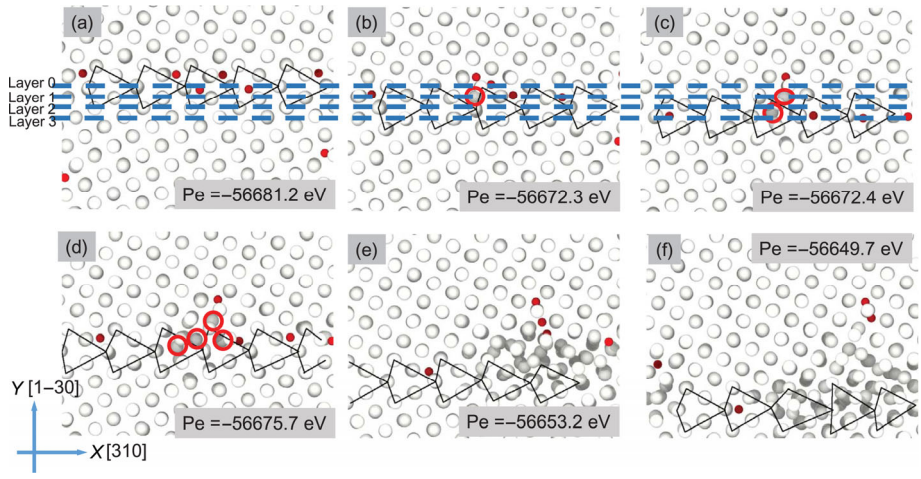

Figure 7 (Color online) Snapshots of the GB structure under applied shear strain with an H concentration of 17 at.%. The larger white spheres indicate W atoms and the smaller red spheres indicate H atoms. The SIAs are emphasized by the grey spheres. The red open circles indicate the key SIAs. The potential energies of system corresponding to the snapshots are also labeled in each sub-figure. The simulation is performed at a temperature 600 K and a strain rate of 1 m/s.

3.4 Temperature effects on the GB migration with H

The effect of multiple H atoms on the GB migration is also studied under different temperatures. As shown in Figure 8, at low temperatures of 300 and 400 K, the shear stress of the system increases gradually with the time and the critical stress is significantly higher than those in a pure GB system. This behavior may be explained by the GB disordering at different temperatures. The disordering effect could be observed at both 300 and 400 K, but at the higher temperatures ranging from 500 K to 900 K, the GB migrates without obvious disordering despite the same H concentration and the original distribution.

In sect. 3.3, we show that the H atoms in the GB region can lead to the disordering of the GB structure. However, at a high temperature, the H will be more difficult to aggregate and easier to detrap from the vacancy, not facilitating the SIA formation. Thus, the SIA could recombine with the vacancy before an SIA is extruded out, and then the GB can migrate without disordering.

The reason we define the critical stress as the maximum of the stress at the whole time range rather than the average of maximal stresses at each period is as following. In a system with H, the critical stress depends not only on the GB migration barrier, but also on the defects induced by H such as self-interstitial, as shown in Figure 8. In the disordering process, the GB structure cannot recover to a normal one after one period, and the stress cannot be released completely, leading to an increase of the critical stress with increasing time. Under such circumstance, we cannot take the average but the maximal stress instead as the critical stress.

The working temperature of W in the divetor of ITER ranges from 500 K to 1300 K [13]. With the H concentration lower than 10 at.%, under such fusion temperature condition, the disordering will not appear because the disordering is more difficult to occur with lower H concentration (as shown in Figure 6). With the H concentration of about 10 at.% that can be reached in the near-surface layer of W in the actual case [28], the disordering can occur in the GBs. Moreover, the H will segregate into GBs, making the H concentration in GB much higher. According to the simulation results, we can speculate that the disordering will occur even at a high temperature (>900 K) if the H concentration in GB is sufficiently high.

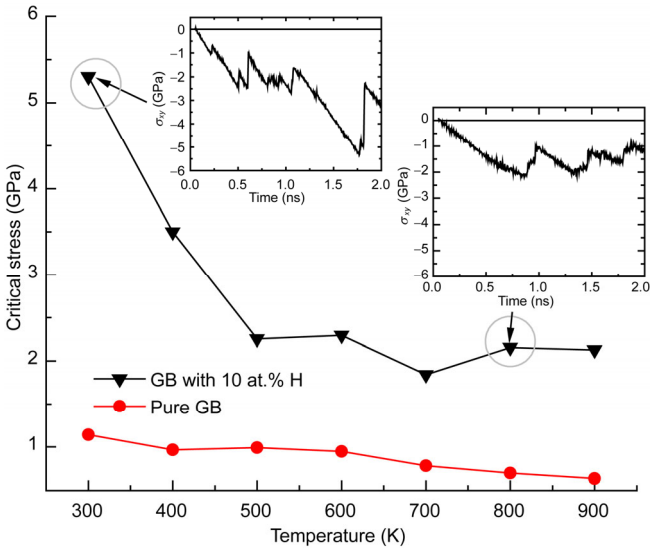

Figure 8 (Color online) Critical stress as a function of temperature without and with H concentration of 10 at.% under the shear deformation with the strain rate of 1 m/s. The insets show the shear stress evolution at the temperature of 300 and 800 K, respectively.

We also performed preliminary simulations to see whether the system can recover to a normal GB structure from the disordered structure through an annealing process. The migration barrier between the disordered GB structure and the normal one is shown to be very high, because the normal GB structure cannot be recovered from the disordered structure even if the annealing temperature arises up to 1000 K. This clearly demonstrates that the disordering is not a restorable process.

3.5 Discussion

Our simulation shows that the H-GB interaction will block the GB migration, which should be determined by the H concentration, the temperature and the migration speed of GB. We can manipulate these factors to reduce the influence of H to the GB migration to facilitate the GB migration. For example, we can increase the migration speed of GB to avoid the H atoms to move along with the GB migration, and thus H in the GB region will not accumulate. Also, we can heat the system to prevent the GB structure from the disordering.

It should be noted that the H-GB interaction energy is overestimated in the present calculation, which is originated from the present W-H atomic potential. The solution energy of H in the GB is calculated to be –2.5 eV, much lower than that from the DFT calculation (–1.2 eV) [42,48]. The overestimated H-GB interaction leads to the overestimated potential energy with H at the GB (more negative), but the potential energy with H far from GB remains unchanged. This makes the potential energy difference with and without H at the GB become larger. As a result, the stress with H at the GB is overestimated as well. Because H binds stronger with GB and thus the H concentration at the GB becomes higher with such overestimated potential, the disordering structure should be easier to form.

4 Conclusions

We have investigated the effects of hydrogen (H) on the migration of grain boundary (GB) in tungsten (W) under different temperatures and H concentrations using a molecular dynamics simulation, motivated by a grain boundary

(GB) healing mechanism that the GB turns into a mobile sink through migration to eliminate the vacancies in a bulk. The shear stress and the structure deformation of the GB system are analyzed. The effects of a single H on the W GB migration under different temperatures show that the H can block the GB migration and increase the friction of the GB migration by pining some nearby W atoms. We demonstrate that the H will follow the GB-migration when the temperature is higher than 300 K. For the case of multiple H in a GB system, the critical stress is shown to increase with the increasing H concentration. In addition to the blocking effect, the H atoms can lead to the emission of self-interstitial atoms (SIAs) in the GB plane when the H concentration is higher than 13 at.% at 600 K. These SIAs will finally form clusters and lead to a disordering of GB structure, and such disordering could significantly increase the critical stress for the GB migration. Moreover, both the critical stress and the probability of GB disordering decrease with the rising temperature. The results provide a useful reference for the possible self-healing effect in W under a fusion environment.

This work was supported by the National Magnetic Confinement Fusion Program (Grant No. 2013GB109002) and the National Natural Science Foundation of China (Grant Nos. 51171008 and 51325103).

1 van Swygenhoven H. Grain boundaries and dislocations. Science, 2002, 296: 66–68
2 Feltham P. Grain growth in metals. Acta Metall, 1957, 5: 97–105
3 Gleiter H. Grain boundaries as point defect sources or sinks—Diffusional creep. Acta Metall, 1979, 27: 187–192
4 Bai X M, Voter A F, Hoagland R G, et al. Efficient annealing of radiation damage near grain boundaries via interstitial emission. Science, 2010, 327: 1631–1634
5 Li X, Liu W, Xu Y, et al. An energetic and kinetic perspective of the grain-boundary role in healing radiation damage in tungsten. Nucl Fusion, 2013, 53: 123014
6 Ackland G. Controlling radiation damage. Science, 2010, 327: 1587–1588
7 Rieth M, Dudarev S L, Gonzalez de Vicente S M, et al. Recent progress in research on tungsten materials for nuclear fusion applications in Europe. J Nucl Mater, 2013, 432: 482–500
8 Borovikov V, Tang X Z, Perez D, et al. Coupled motion of grain boundaries in bcc tungsten as a possible radiation-damage healing mechanism under fusion reactor conditions. Nucl Fusion, 2013, 53: 063001
9 Ivanov V A, Mishin Y. Dynamics of grain boundary motion coupled to shear deformation: An analytical model and its verification by molecular dynamics. Phys Rev B, 2008, 78: 064106
10 Rupert T J, Gianola D S, Gan Y, et al. Experimental observations of stress-driven grain boundary migration. Science, 2009, 326: 1686–1690
11 Balluffi R. Grain boundary diffusion mechanisms in metals. J Electron Mater, 1992, 21: 527–553
12 Cahn J W, Taylor J E. A unified approach to motion of grain boundaries, relative tangential translation along grain boundaries, and grain rotation. Acta Mater, 2004, 52: 4887–4898
13 Bolt H, Barabash V, Federici G, et al. Plasma facing and high heat flux materials – needs for ITER and beyond. J Nucl Mater, 2002, 307-311: 43–52
14 Gorkaya T, Burlet T, Molodov D A, et al. Experimental method for true *in situ* measurements of shear-coupled grain boundary migration. Scr Mater, 2010, 63: 633–636
15 Janeschitz G. Plasma–wall interaction issues in ITER. J Nucl Mater, 2001, 290-293: 1–11
16 Liu Y N, Ahlgren T, Bukonte L, et al. Mechanism of vacancy formation induced by hydrogen in tungsten. AIP Adv, 2013, 3: 122111
17 Yang X, Hassanein A. Molecular dynamics simulation of deuterium trapping and bubble formation in tungsten. J Nucl Mater, 2013, 434: 1–6
18 Xiao W, Geng W T. Role of grain boundary and dislocation loop in H blistering in W: A density functional theory assessment. J Nucl Mater, 2012, 430: 132–136
19 Zhou H B, Liu Y L, Jin S, et al. Investigating behaviours of hydrogen in a tungsten grain boundary by first principles: From dissolution and diffusion to a trapping mechanism. Nucl Fusion, 2010, 50: 025016
20 Liu Y L, Zhang Y, Zhou H B, et al. Vacancy trapping mechanism for hydrogen bubble formation in metal. Phys Rev B, 2009, 79: 172103
21 Zhou H B, Jin S, Zhang Y, et al. Anisotropic strain enhanced hydrogen solubility in bcc metals: The independence on the sign of strain. Phys Rev Lett, 2012, 109: 135502
22 Liu Y L, Zhou H B, Jin S, et al. Effects of H on electronic structure and ideal tensile strength of W: A first-principles calculation. Chin Phys Lett, 2010, 27: 127101
23 Liu Y L, Zhang Y, Luo G N, et al. Structure, stability and diffusion of hydrogen in tungsten: A first-principles study. J Nucl Mater, 2009, 390: 1032–1034
24 Lu G H, Zhou H B, Becquart C S. A review of modelling and simulation of hydrogen behaviour in tungsten at different scales. Nucl Fusion, 2014, 54: 086001
25 Liu Y L, Ma Y, Dai Z H, et al. A possible critical temperature mechanism for H blistering nucleation/dissociation in metals. Solid State Commun, 2015, 201: 43–48
26 Liu Y L, Shi W. Investigating permeation and transport of H isotopes in tungsten by first-principles. Fusion Eng Des, 2013, 88: 368–373
27 Zhou H B, Jin S, Yan W L. Effects of hydrogen in a vanadium grain boundary: From site occupancy to mechanical properties. Sci China-Phys Mech Astron, 2013, 56: 1389–1395
28 Alimov V K, Roth J. Hydrogen isotope retention in plasma-facing materials: Review of recent experimental results. Phys Scr, 2007, T128: 6–13
29 Haasz A A, Davis J W, Poon M, et al. Deuterium retention in tungsten for fusion use. J Nucl Mater, 1998, 258: 889–895
30 Tokunaga K, Baldwin M J, Doerner R P, et al. Blister formation and deuterium retention on tungsten exposed to low energy and high flux deuterium plasma. J Nucl Mater, 2005, 337: 887–891
31 Nishijima D, Iwakiri H, Amano K, et al. Suppression of blister formation and deuterium retention on tungsten surface due to mechanical polishing and helium pre-exposure. Nucl Fusion, 2005, 45: 669–674
32 Ogorodnikova O V, Roth J, Mayer M. Deuterium retention in tungsten in dependence of the surface conditions. J Nucl Mater, 2003, 313-316: 469–477
33 Roth J, Schmid K, Joachim R, et al. Hydrogen in tungsten as plasma-facing material. Phys Scr, 2011, T145: 14031
34 Shu W M, Luo G N, Yamanishi T. Mechanisms of retention and blistering in near-surface region of tungsten exposed to high flux deuterium plasmas of tens of eV. J Nucl Mater, 2007, 367-370: 1463–1467
35 Ye M Y, Kanehara H, Fukuta S, et al. Blister formation on tungsten surface under low energy and high flux hydrogen plasma irradiation in NAGDIS-I. J Nucl Mater, 2003, 313-316: 72–76
36 Luo G N, Shu W M, Nishi M. Influence of blistering on deuterium retention in tungsten irradiated by high flux deuterium 10–100 eV plasmas. Fusion Eng Des, 2006, 81: 957–962

37 Johnson D F, Carter E A. Hydrogen in tungsten: Absorption, diffusion, vacancy trapping, and decohesion. J Mater Res, 2011, 25: 315–327
38 Terentyev D, Dubinko V, Bakaev A, et al. Dislocations mediate hydrogen retention in tungsten. Nucl Fusion, 2014, 54: 042004
39 Haasz A A, Poon M, Davis J W. The effect of ion damage on deuterium trapping in tungsten. J Nucl Mater, 1999, 266: 520–525
40 Plimpton S. Fast parallel algorithms for short-range molecular dynamics. J Comput Phys, 1995, 117: 1–19
41 Li X C, Shu X, Liu Y N, et al. Modified analytical interatomic potential for a W–H system with defects. J Nucl Mater, 2011, 408: 12–17
42 Yu Y, Shu X, Liu Y N, et al. Molecular dynamics simulation of hydrogen dissolution and diffusion in a tungsten grain boundary. J Nucl Mater, 2014, 455: 91–95
43 Huang B W, Shang J X, Liu Z H, et al. Atomic simulation of bcc niobium sigma5(310)grain boundary under shear deformation. Acta Mater, 2014, 77: 258–268
44 Yu Y, Shu X, Lu G H. Dependence of critical stress on temperature and shear strain rate in grain boundary of W. Mater Res Innov, 2014, 18: 1078–1081
45 Juslin N, Wirth B D. Interatomic potentials for simulation of He bubble formation in W. J Nucl Mater, 2013, 432: 61–66
46 Heitjans P, Kärger J. Diffusion in Condensed Matter. Heidelberg: Springer, 2005. 745–792
47 Liu Y N, Wu T, Yu Y, et al. Hydrogen diffusion in tungsten: A molecular dynamics study. J Nucl Mater, 2014, 455: 676–680
48 Sun L, Jin S, Li X C, et al. Hydrogen behaviors in molybdenum and tungsten and a generic vacancy trapping mechanism for H bubble formation. J Nucl Mater, 2013, 434: 395–401